

# Earth matter effects in supernova neutrinos: Optimal detector locations

A. Mirizzi<sup>1</sup>, G.G. Raffelt<sup>2</sup> and P.D. Serpico<sup>2</sup>

<sup>1</sup> Dipartimento di Fisica and Sezione INFN di Bari, Via Amendola 173, 70126 Bari, Italy

<sup>2</sup> Max-Planck-Institut für Physik (Werner-Heisenberg-Institut), Föhringer Ring 6, 80805 München, Germany

E-mail: alessandro.mirizzi@ba.infn.it, raffelt@mppmu.mpg.de, and serpico@mppmu.mpg.de

**Abstract.** A model-independent experimental signature for flavor oscillations in the neutrino signal from the next Galactic supernova (SN) would be the observation of Earth matter effects. We calculate the probability for observing a Galactic SN shadowed by the Earth as a function of the detector's geographic latitude. This probability depends only mildly on details of the Galactic SN distribution. A location at the North Pole would be optimal with a shadowing probability of about 60%, but a far-northern location such as Pyhäsalmi in Finland, the proposed site for a large-volume scintillator detector, is almost equivalent (58%). We also consider several pairs of detector locations and calculate the probability that only one of them is shadowed, allowing a comparison between a shadowed and a direct signal. For the South Pole combined with Kamioka this probability is almost 75%, for the South Pole combined with Pyhäsalmi it is almost 90%. One particular scenario consists of a large-volume scintillator detector located in Pyhäsalmi to measure the geo-neutrino flux in a continental location and another such detector in Hawaii to measure it in an oceanic location. The probability that only one of them is shadowed exceeds 50% whereas the probability that at least one is shadowed is about 80%. We provide an online tool to calculate different shadowing probabilities for the one- and two-detector cases.

*Keywords:* Supernova neutrinos, neutrino detectors

PACS numbers: 97.60.Bw, 14.60.Pq, 95.55.Vj

## 1. Introduction

Galactic core-collapse supernovae are rare, perhaps a few per century [1, 2]. However, the large number of existing or future neutrino detectors with a broad range of science goals almost guarantees continuous exposure for several decades, so that a high-statistics supernova (SN) neutrino signal may eventually be observed. Such a measurement would provide a plethora of new insights that are crucial both for our astrophysical understanding of the core-collapse phenomenon [3] and for using SNe as particle-physics laboratories [4]. Of particular interest would be the observation of signatures for flavor oscillations because this could address a key question of neutrino physics, i.e. whether the neutrino masses are ordered in a normal or inverted hierarchy [5, 6, 7, 8, 9, 10].

The collapsed core of a SN emits neutrinos and anti-neutrinos of all flavors with comparable fluxes and spectra [11, 12, 13, 14]. One expects differences between the spectra and fluxes of  $\bar{\nu}_e$  and  $\bar{\nu}_{\mu,\tau}$  or between  $\nu_e$  and  $\nu_{\mu,\tau}$  that are large enough to observe flavor oscillations, but it will be difficult to establish such effects solely on the basis of a  $\bar{\nu}_e$  or  $\nu_e$  “spectral hardening” relative to theoretical expectations. Therefore, in the recent literature the importance of model-independent signatures has been emphasized, e.g. in association with the prompt  $\nu_e$  neutronization burst [15] or with shock-wave propagation [16, 17, 18, 19]. One unequivocal signature would be the observation of Earth matter effects, because they induce a characteristic energy-dependent modulation on the measured flux [6, 7, 8, 20, 21]. In a large-volume liquid scintillator detector such as the proposed 50 kt Low Energy Neutrino Astronomy (LENA) project [22] this modulation could be detected with high statistical significance [20]. Moreover, even if single detectors can not resolve these modulations, comparing the signals from a shadowed with an unshadowed detector may allow one to diagnose Earth effects [8].

These intriguing possibilities have motivated us to investigate the probability for given detector locations to observe the next Galactic SN in an Earth-shadowed position. Most of the Milky Way is in the southern sky so that a northern location is obviously preferred, but a quantitative determination of the probability distribution of Earth-shadowing as a function of geographic latitude is missing, except for a brief discussion in Ref. [6]. An additional motivation for our work is that large-volume scintillator detectors are being discussed for the purpose of geo-neutrino observations. After KamLAND’s pioneering measurement of the  $\bar{\nu}_e$  flux from uranium and thorium  $\beta$ -decays in the Earth [23], performed in a complex geophysical environment with a large  $\bar{\nu}_e$  background from power reactors, the exploration of different detector sites has become crucial. The choice of location could be influenced by the role of such detectors as excellent SN neutrino observatories, in particular because they need to operate for a long time to accumulate meaningful statistics for geo-neutrino studies. For example, if a large-volume scintillator detector were built in the Pyhäsalmi mine (Finland) [24] to measure the geo-neutrino flux mainly from the continental crust and another one in Hawaii [25] to measure neutrinos from the oceanic crust, the “geographic complementarity” of these locations with regard to SN shadowing is important.

We begin in Sec. 2 with a discussion of the distribution of core-collapse SNe in the Galaxy and then determine the SN probability distribution in the sky. In Sec. 3 we determine the probability for Earth shadowing as a function of geographic location of one or two detectors. We also provide an online tool for the calculation of these probabilities [26]. We conclude our work in Sec. 4.

## 2. Supernova distribution in the Milky Way

In this section we characterize the SN probability distribution in our Galaxy. In Sec. 2.1 we present the models adopted for the SN volume distribution. In Sec. 2.2 we discuss the probability of a core-collapse SN in terms of Galactic and Equatorial coordinates. Finally in Sec. 2.3 we estimate the distance distribution of SN events. The SN distribution in the Galaxy is expressed in cylindrical galactocentric coordinates  $(r, z, \theta)$ , where the origin corresponds to the Galactic center,  $r$  indicates the radial coordinate,  $\theta$  the azimuthal angle and  $z$  the height with respect to the Galactic plane.

### 2.1. Models for the volume distribution

The probability distribution of core-collapse SNe in the Milky Way is not well known. These SNe mark the final evolution of massive stars and thus must occur in regions of active star formation, i.e. in the Galactic spiral arms. As proxies for the core-collapse SN distribution one can use either observations of other Galaxies, or in our Galaxy the distribution of pulsars and SN remnants (SNRs), the distribution of molecular hydrogen ( $\text{H}_2$ ) and ionized hydrogen (HII) and the distribution of OB-star formation regions. (For a review see Ref. [27] and references there.) These observables are either directly connected with core-collapse events (SNRs, pulsars) or with young, massive star formation activity and the related emission of ultraviolet light ( $\text{H}_2$ , HII, OB stars). All of these observables are consistent with a deficit of SNe in the inner Galaxy and a maximum of the probability at 3.0–5.5 kpc galactocentric distance.

The star formation activity is not smoothly distributed in the Galaxy. Besides generally following the spiral arms, it can be concentrated in small regions or spike-like complexes like the Cygnus OB association. Small regions of high star-forming activity have also been found within 50 pc from the Galactic center [28] that may contribute up to 1% of the total Galactic star formation rate, although this finding does not seem to contradict the overall picture of a reduced SN rate in the inner Galaxy.

However, we are only interested in the SN distribution projected on the sky and the Earth's rotation introduces an additional averaging effect. Therefore, it will be enough to consider a smooth distribution with azimuthal symmetry. In particular, we shall use the following common parametrization for the Galactic surface density of core-collapse (cc) events,

$$\sigma_{\text{cc}}(r) \propto r^\xi \exp(-r/u) , \quad (1)$$

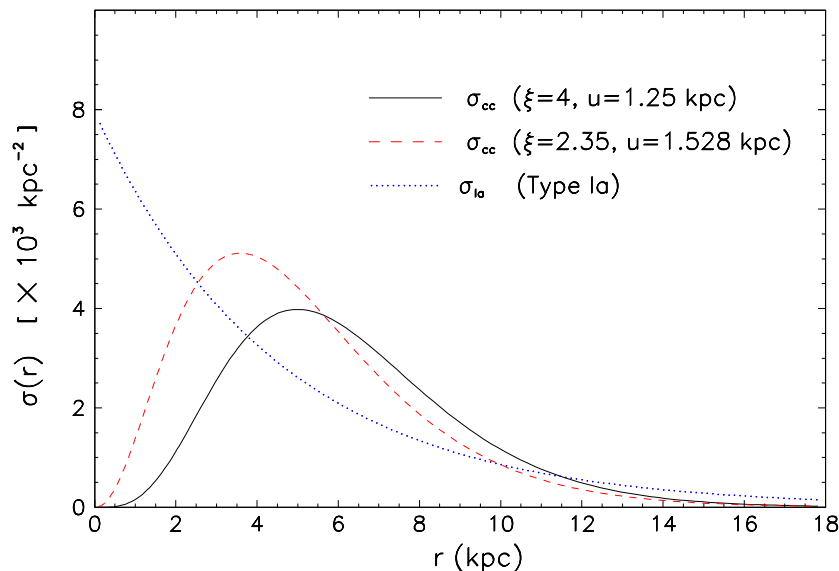


**Figure 1.** Galactic surface density of core-collapse SNe as a function of galactocentric radius according to Eq. (1). *Solid curve:* Our benchmark case with the parameters of Eq. (2). *Dashed curve:* Alternative parameters of Eq. (3). *Dotted curve:* Type Ia SNe according to Eq. (6). The surface densities are normalized as  $\int \sigma(r) 2\pi r dr = 1$ .

where  $r$  is the galactocentric radius. For the birth location of neutron stars, a fiducial distribution of this form was suggested with the parameters [29]

$$\text{Neutron stars:} \quad \begin{cases} \xi = 4, \\ u = 1.25 \text{ kpc}. \end{cases} \quad (2)$$

These parameters are consistent with several SN-related observables, even though large uncertainties remain [29]. On the other hand, the pulsar distribution indicates [30]

$$\text{Pulsars:} \quad \begin{cases} \xi = 2.35, \\ u = 1.528 \text{ kpc}. \end{cases} \quad (3)$$

We will use the parameters of Eq. (2) as our benchmark values and those of Eq. (3) as an alternative model to illustrate the dependence of our results on different input choices.

In Fig. 1 we show the normalized Galactic surface density of core-collapse SNe according to Eq. (1) as a function of the galactocentric distance for the two choices of parameters given in Eqs. (2) and (3). Our benchmark distribution shows a peak at  $r = 5$  kpc, while for the parameters of Eq. (3) the surface density peaks at a lower distance  $r \simeq 3$  kpc. The distributions are normalized as  $\int dr \sigma(r) 2\pi r = 1$ , i.e. the surface densities  $\sigma$  are given in SNe per  $\text{kpc}^2$ . Of course, to obtain the number of SN events per Galactic unit surface and unit time, the quantities  $\sigma$  would have to be multiplied with the integrated Galactic SN rate. However, since we are only interested in the relative probability of SNe in different regions of the sky, the overall rate is not important for our study.

The vertical distribution of neutron stars at birth with respect to the Galactic plane can be approximated by the superposition of a thin Gaussian disk with a scale height of 212 pc and a thick disk with three times this scale height, containing 55% and 45% of the pulsars, respectively [27],

$$\mathcal{R}_{\text{cc}}(z) \propto 0.79 \exp \left[ - \left( \frac{z}{212 \text{ pc}} \right)^2 \right] + 0.21 \exp \left[ - \left( \frac{z}{636 \text{ pc}} \right)^2 \right], \quad (4)$$

where  $z$  is the height above the Galactic plane. We assume this vertical distribution to be independent of galactocentric distance [30] so that

$$n_{\text{cc}}(r, z) \propto \sigma_{\text{cc}}(r) \mathcal{R}_{\text{cc}}(z) \quad (5)$$

is the volume distribution.

We stress that the distribution of core-collapse SNe differs significantly from the overall matter distribution, particularly in the inner part of the Galaxy. The distribution of Type Ia SNe—that are believed to originate from old stars in binary systems—more closely follows the matter distribution. It can be parameterized as [27]

$$n_{\text{Ia}}(r, z) = \sigma_{\text{Ia}}(r) \mathcal{R}_{\text{Ia}}(z) \propto \exp \left( - \frac{r}{4.5 \text{ kpc}} \right) \exp \left( - \frac{|z|}{325 \text{ pc}} \right). \quad (6)$$

In Fig. 1 we show the monotonically falling SNe Ia surface density  $\sigma_{\text{Ia}}(r)$  for comparison with the core-collapse case.

## 2.2. Projection on the sky

The probability of a core-collapse SN as a function of the Galactic longitude  $l$  and latitude  $b$  is given by an integration along the line of sight,

$$P(l, b) \propto \int_0^\infty ds n_{\text{cc}}[r(s, l, b), z(s, b)], \quad (7)$$

where

$$\begin{aligned} r &= \left( s^2 \cos^2 b + d_\odot^2 - 2 s d_\odot \cos l \cos b \right)^{1/2}, \\ z &= s \sin b. \end{aligned} \quad (8)$$

Here,  $-\pi \leq l \leq \pi$ ,  $-\pi/2 \leq b \leq \pi/2$ , and  $d_\odot \simeq 8.5 \text{ kpc}$  is the solar distance from the Galactic center. The function  $P(l, b)$  can be recast in terms of the Equatorial coordinates  $(\alpha, \delta)$ , in which the reference plane is the Earth equator instead of the Galactic plane. The transformation relating the two systems of coordinates is

$$\sin \delta = \sin b \sin \delta_{\text{NGP}} + \cos b \cos \delta_{\text{NGP}} \sin(l - l_0), \quad (9)$$

$$\cos(\alpha - \alpha_0) = \cos(l - l_0) \cos b / \cos \delta, \quad (10)$$

$$\sin(\alpha - \alpha_0) = [-\sin b \cos \delta_{\text{NGP}} + \cos b \sin \delta_{\text{NGP}} \sin(l - l_0)] / \cos \delta, \quad (11)$$

where, for the Julian epoch J2000, the coordinates of the north Galactic pole (NGP) are  $\alpha_{\text{NGP}} = 12 \text{ h } 51.42 \text{ m}$  and  $\delta_{\text{NGP}} = 27^\circ 07.8'$ . Hence, the ascending node of the Galactic equator is at  $\alpha_0 = 282.86^\circ$  and  $l_0 = 32.93^\circ$ . Further details on astronomical coordinate systems can be found, for example, in Ref. [31].

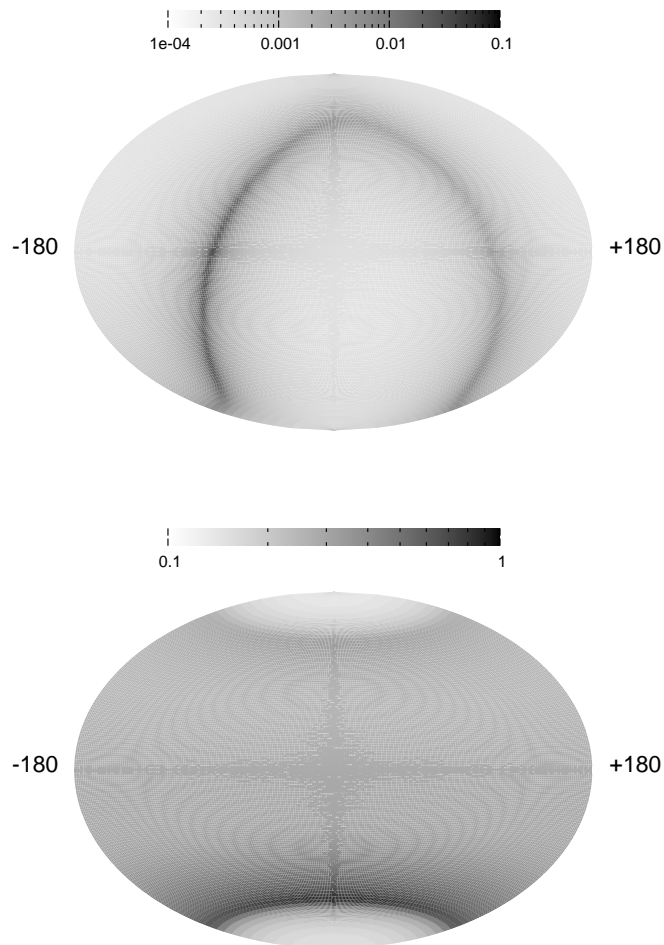


**Figure 2.** Probability distribution  $P(\alpha, \delta)$  of core-collapse SNe in the sky. *Top:* Earth Equatorial coordinates. *Bottom:* Average over right-ascension, see Eq. (12).

The sky map in Equatorial coordinates is shown in the upper panel of Fig. 2 for our benchmark distribution. However, since the neutrino detectors are fixed to the Earth, we only need this distribution averaged over time, i.e. over right ascension  $\alpha$ . Therefore, all relevant information is contained in the “exposure probability function”

$$\omega(\delta) \propto \int_{-\pi}^{+\pi} d\alpha P(\alpha, \delta). \quad (12)$$

It provides the probability distribution of the arrival direction of a SN signal in terms of declination. We show the time-averaged sky map in the bottom panel of Fig. 2, normalized as  $\int d\delta \omega(\delta) \cos \delta = 1$ . This normalization also fixes the overall constant for the function  $P(\alpha, \delta)$  plotted in the top panel of Fig. 2. Fig. 2 clearly shows the preference of southern locations in the sky and also shows the polar regions that are nearly void of SNe because the Milky Way extends approximately between declinations of  $-60^\circ$  to  $+60^\circ$ .

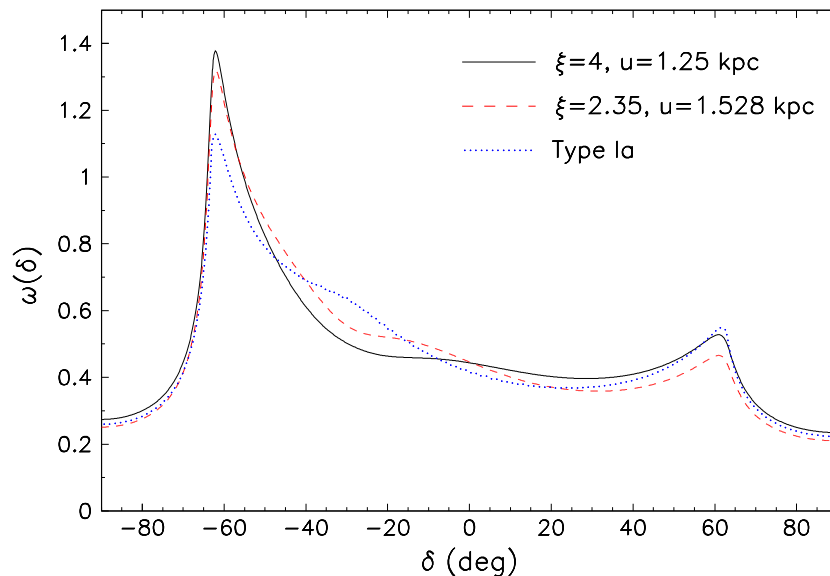


**Figure 3.** The “exposure function”  $\omega(\delta)$  for different Galactic SNe distributions. *Solid curve:* Benchmark model based on Eq. (1) with the parameters of Eq. (2). *Dashed curve:* Same with the alternative parameters of Eq. (3). *Dotted curve:* Distribution of SNe Ia for comparison.

In Fig. 3 we show the exposure probability function  $\omega(\delta)$  for different assumptions about the Galactic SN distribution, i.e. our benchmark distribution Eq. (1) with the parameters of Eq. (2), the alternative parameters of Eq. (3), and as an extreme case the SN Ia distribution of Eq. (6) which, of course, is not realistic for core-collapse SNe. The normalization  $\int d\delta \omega(\delta) \cos \delta = 1$  is adopted throughout. In this normalization of  $\omega(\delta)$  an isotropic SN distribution would correspond to a horizontal line in Fig. 3. The exposure function depends only mildly on details of the assumed Galactic SN distribution, because the geometric effect dominates that the SN probability is negligible outside the Galactic disk. The largest model variation occurs around a declination of  $-30^\circ$  near the Galactic center region. The edges at about  $\pm 60^\circ$  correspond to the region where the Milky Way would end in the sky if it were infinitely thin. The tails beyond these declinations come from the vertical extension of the Galactic disk around us where we have assumed the solar system to be located exactly in the Galactic plane.

### 2.3. Distance distribution

As an aside, we use our assumed core-collapse SN distribution in the Galaxy to evaluate the SN distance distribution relative to the solar system. The average distance is

$$\langle d_{cc} \rangle = \frac{\int n_{cc}(r, z) d(r, z, \theta) r dr dz d\theta}{\int n_{cc}(r, z) 2\pi r dr dz}, \quad (13)$$

where

$$d(r, z, \theta) = \left[ (x - x_\odot)^2 + (y - y_\odot)^2 + (z - z_\odot)^2 \right]^{1/2}$$

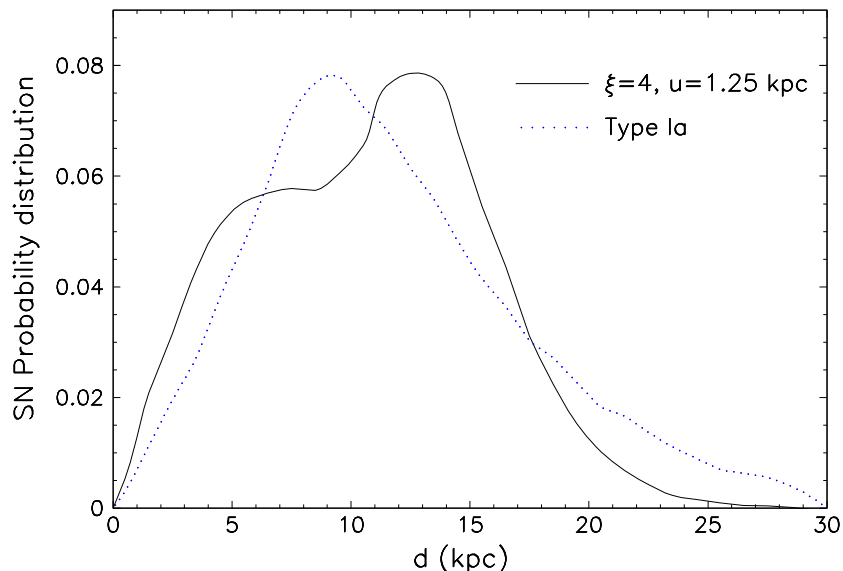


**Figure 4.** SN probability vs. distance from the Sun. *Solid curve:* Benchmark model based on Eqs. (1) and (2). *Dotted curve:* SNe Ia assuming Eq. (6).

$$= \left[ r^2 + z^2 + d_{\odot}^2 - 2rd_{\odot} \cos \theta \right]^{1/2}. \quad (14)$$

For the distribution  $n_{cc}$  of Eq. (5) with our benchmark parameters of Eq. (2) we find  $\langle d_{cc} \rangle = 10.7$  kpc with a rms dispersion of 4.9 kpc. While the average distance agrees with the fiducial distance of 10 kpc that is frequently assumed in the literature, we note that the dispersion of distances is very large. This is clearly visible in Fig. 4 where we plot the probability distribution  $\Pi(d)$  of SN events as a function of the distance  $d$  from the Sun, so that  $\int_a^b \Pi(x) dx$  gives the probability that a SN happens between distance  $a$  and  $b$  from the Sun. The dip in the middle corresponds to the deficit of core-collapse SNe in the Galactic center region. For comparison we also show the probability distribution for SNe Ia according to Eq. (6). Their average distance is 11.9 kpc with a rms dispersion of 6.0 kpc. On the other hand, the median distances are quite similar for the two distributions, and equal to about 10.9 kpc. The large-distance behavior for both cases differs significantly due to the different scales in the exponential tails of Eqs. (1) and (6). Of course, the scarcity of data at large galactocentric distances implies that the extrapolation may be unphysical.

### 3. Optimal detector location

#### 3.1. One detector

Armed with the exposure function  $\omega(\delta)$  shown in Fig. 3 we now determine the probability that a detector located at a geographic latitude  $\lambda$  will observe the next Galactic SN below the Earth horizon. Of course, observable matter effects would require a minimal path-length of a few thousand kilometers [20] so that our Earth-shadowing criterion is



somewhat schematic. Moreover, the phenomenological signature of Earth matter effects also depends on whether or not the neutrinos cross the core [21, 32, 33]. We use a core radius  $R_c = 3486$  km and an Earth radius of  $R_\oplus = 6371$  km [34]. The Earth or core shadowing condition for a source with altitude  $a$  with respect to the horizon is

$$\sin a < \kappa = \begin{cases} 0, & \text{Earth shadowing,} \\ -\sin a_c, & \text{Core shadowing,} \end{cases} \quad (15)$$

where

$$\sin a_c = \sqrt{1 - (R_c/R_\oplus)^2} = 0.837. \quad (16)$$

In general, for a neutrino path-length  $L$  in the Earth, one has

$$\kappa = -\sin a_L = -\frac{L}{2R_\oplus}. \quad (17)$$

The altitude of an object of equatorial coordinates  $(\alpha, \delta)$  is

$$\sin a = \sin \lambda \sin \delta + \cos \lambda \cos \delta \cos H, \quad (18)$$

where  $H = t - \alpha$  is the hour angle and  $t$  the local sidereal time. Since no time information on the next SN is available in advance,  $H$  has to be taken as a random variable.

For polar locations ( $\lambda = \pm \pi/2$ ) the shadowing condition simplifies, because  $\cos \lambda = 0$  and the time dependence disappears. The geometrical probability  $p_\kappa(\lambda, \delta)$  for a trajectory to satisfy one of the shadowing conditions is

$$p_\kappa\left(\pm \frac{\pi}{2}, \delta\right) = \Theta(\kappa \mp \sin \delta), \quad (19)$$

where  $\Theta(x)$  is the usual step function. A similar simplification holds for objects located at the celestial poles ( $\delta = \pm \pi/2$ ) for which  $\sin a = \pm \sin \lambda$  and

$$p_\kappa\left(\lambda, \pm \frac{\pi}{2}\right) = \Theta(\kappa \mp \sin \lambda). \quad (20)$$

Equation (20) is related to Eq. (19) by the symmetry  $p_\kappa(\lambda, \delta) = p_\kappa(\delta, \lambda)$ . This is a general property following directly from Eq. (18).

Apart from these special cases, we have both  $\cos \lambda > 0$  and  $\cos \delta > 0$  so that the general shadowing condition Eq. (15) can be recast as

$$\cos H < -\tan \lambda \tan \delta + \frac{\kappa}{\cos \lambda \cos \delta}, \quad (21)$$

or equivalently

$$\cos H > \tan \lambda \tan \delta - \frac{\kappa}{\cos \lambda \cos \delta} \equiv h_\kappa(\lambda, \delta). \quad (22)$$

Note that we have replaced  $H + \pi$  with  $H$  in the argument of the cosine, since both are random variables. Unless Eq. (22) is always or never satisfied, one has

$$-\arccos h_\kappa(\lambda, \delta) < H \pmod{2\pi} < \arccos h_\kappa(\lambda, \delta). \quad (23)$$

The general solution is then

$$p_\kappa(\lambda, \delta) = \begin{cases} \Theta[1 - h_\kappa(\lambda, \delta)] \Theta[-h_\kappa(\lambda, \delta) - 1] & \text{for } |h_\kappa(\lambda, \delta)| \geq 1, \\ \frac{1}{\pi} \arccos h_\kappa(\lambda, \delta) & \text{otherwise.} \end{cases} \quad (24)$$

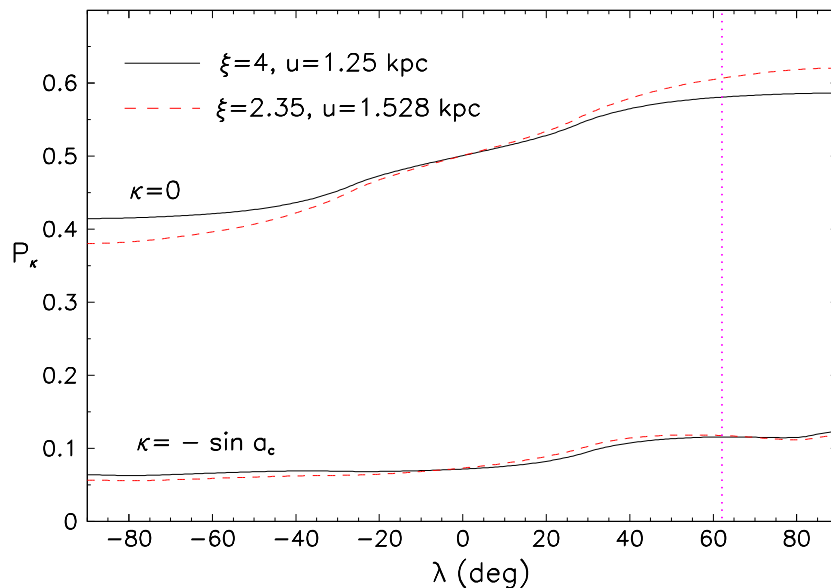


**Figure 5.** Probability for Earth shadowing (upper curves) and core shadowing (lower curves). *Solid lines:* Galactic benchmark distribution with parameters given by Eq. (2). *Dashed lines:* Alternative parameters of Eq. (3). The latitude of the Pyhäsalmi site is indicated by the vertical dotted line.

This follows because all values of the random variable  $H(\text{mod } 2\pi)$  in the interval  $(-\pi, \pi]$  are equally likely. As a check of Eq. (24) we note that for a detector at the equator ( $\lambda = 0$ ) it simplifies to

$$p_\kappa(0, \delta) = \frac{1}{\pi} \arccos\left(\frac{\kappa}{\cos \delta}\right), \quad (25)$$

reproducing the trivial result  $p_0(0, \delta) = 1/2$ .

In order to obtain the Earth shadowing probability for the neutrinos from the next Galactic SN, given the detector latitude  $\lambda$ , we must convolve with the distribution of source declination angles, i.e. with the exposure function, so that

$$P_\kappa(\lambda) = \int d\delta \cos \delta p_\kappa(\lambda, \delta) \omega(\delta), \quad (26)$$

where we have used the normalization  $\int d\delta \cos \delta \omega(\delta) = 1$ .

We show the Earth and core shadowing probability as a function of detector latitude in Fig. 5. The solid lines refer to our Galactic benchmark distribution Eq. (1) with parameters Eq. (2) whereas the dashed lines refer to the alternative parameters Eq. (3). Once more we find that the dependence on details of the Galactic distribution is mild. Note that for the Earth-shadowing case  $P_0(\lambda) + P_0(-\lambda) = 1$  because all information on the longitude is lost and two locations at  $\lambda$  and  $-\lambda$  are complementary: if one detector is shadowed, the antipodal one is certain not to be shadowed.

The largest probability for Earth shadowing is at the North pole, but the Pyhäsalmi site in Finland is almost equivalent. The behavior for the core shadowing condition is similar, although the advantage of a northern site is somewhat boosted: for  $\kappa = -\sin a_c$ ,

**Table 1.** Representative locations of proposed or existing SN neutrino detectors and neutrino shadowing probabilities, assuming our benchmark Galactic distribution.

Location	Latitude	Longitude	Shadowing probability	
			Earth	Core
Pyhäsalmi, Finland	63.66° N	26.04° E	0.581	0.116
Soudan, USA	47.82° N	92.23° W	0.572	0.112
Fréjus, France-Italy	43.43° N	6.73° E	0.568	0.110
Kamioka, Japan	36.27° N	137.3° E	0.560	0.104
Hawaii, USA	19.70° N	156.30° W	0.528	0.082
Sydney, Australia	33.87° S	151.22° E	0.445	0.069
South Pole	90° S	—	0.414	0.064

the probability  $P_\kappa(\lambda)$  varies by almost a factor two moving from a far-southern location to a far-northern one, where it reaches almost 12%. If one asks for a minimal neutrino path-length of  $L = 3000$  km [20], the shadowing probability is about 10% less than the shown Earth-crossing case. However, the minimum path-length to detect Earth signatures depends on the detailed features of the flavor-dependent neutrino fluxes and on the detector properties. Therefore, to keep our discussion simple and general we restrict ourselves to the illustrative cases of Earth and core crossing. Note that the generic case can be calculated with the online tool [26].

Some representative locations are tabulated in Table 1. The list is not exhaustive, but rather meant to provide representative and complementary geographic locations. It includes two existing locations of high-statistics experiments sensitive to SN neutrinos, i.e. Super-Kamiokande in Japan [35] and IceCube that is under construction at the South Pole [36], and a few possible locations of next-generation detectors proposed in the literature. In particular, the possibility of a Megatonne water-Cherenkov detector is discussed worldwide, including the Underground nucleon decay and Neutrino Observatory (UNO) with a possible location in the Soudan mine (Minnesota, USA) [37], the Hyper-Kamiokande (HK) detector in the Tochibora Mine (Kamioka region, Japan) [38], and the MEGaton class PHYSics (MEMPHYS) detector at the Fréjus site (France-Italy) [39]. Different locations are under study for the large-volume scintillator detector LENA. The Pyhäsalmi mine in Finland and Hawaii are of interest for geo-neutrino studies. Hawaii and Australia have also been discussed as favored sites for detecting the cosmic diffuse SN neutrino background because of the low reactor background [40].

### 3.2. Two detectors

Next we consider the simultaneous SN neutrino detection by two different detectors. A single detector can observe Earth matter effects only if it has good energy resolution and, of course, enough statistics. A scintillator detector like the 50-kton LENA project has good energy resolution and can detect unambiguously these signatures, whereas water

Cherenkov detectors have an intrinsically poorer energy resolution so that Megaton-scale masses would be necessary [20]. However, smaller detectors, even if they can not resolve directly the modulations, could still reveal Earth effects by the comparison of the signals from a shadowed with an unshadowed detector. Of particular interest are Super-Kamiokande in Japan and IceCube at the South Pole that will be completed in a few years. In this case the Earth effect will be detected as a difference in the signal normalization between the two detectors [8]. To this end it would be crucial that one of the detectors is shadowed whereas the other is not, i.e. we are interested in the probability for exactly one of them to be shadowed.

The special location of IceCube makes this kind of problem a very simple generalization of the previous one-detector case. The shadowing condition of Eq. (15) is satisfied or missed at the South Pole with a probability given by the lower or upper sign of Eq. (19), and at any other location according to Eq. (24) or its complement to 1. Note that we can safely use the formulae of Sec. 3.1 since the location of one detector at the South Pole implies that no longitude difference enters the problem.

In the general case of two detectors at geographic latitudes  $\lambda$  and  $\lambda'$  with a difference in longitude of  $\Delta$ , the altitudes  $a$  and  $a'$  of an object located at  $(\alpha, \delta)$  are

$$\begin{cases} \sin a = \sin \lambda \sin \delta + \cos \lambda \cos \delta \cos H , \\ \sin a' = \sin \lambda' \sin \delta + \cos \lambda' \cos \delta \cos(H + \Delta) . \end{cases} \quad (27)$$

To maximize the chance to detect Earth matter effects, the most interesting case for two general detectors is that exactly one of them sees a SN from a shadowed position, thus allowing one to compare a shadowed signal with an unshadowed one. The probability for detector I to be shadowed and detector II not is: (i) zero if one of the two probabilities vanishes when calculated as described in the previous section; (ii) trivially equal to the one-detector case when the probability of one of the single-detector conditions is 1; (iii) in all remaining cases it can be evaluated from the following system of inequalities where we omit (mod  $2\pi$ )

$$\begin{cases} -\arccos h_\kappa(\lambda, \delta) < H < \arccos h_\kappa(\lambda, \delta) , \\ \arccos h_\kappa(\lambda', \delta) < H + \Delta < 2\pi - \arccos h_\kappa(\lambda', \delta) . \end{cases} \quad (28)$$

The fraction of the  $2\pi$ -angle satisfying the previous conditions is the desired probability. The complementary situation, i.e. detector II is shadowed and detector I not, is

$$\begin{cases} \arccos h_\kappa(\lambda, \delta) < H < 2\pi - \arccos h_\kappa(\lambda, \delta) , \\ -\arccos h_\kappa(\lambda', \delta) < H + \Delta < \arccos h_\kappa(\lambda', \delta) , \end{cases} \quad (29)$$

apart for the trivial cases (i) and (ii) described above.

It is also worthwhile to consider the situation that two detectors with excellent energy resolution are available, e.g. two scintillator detectors. We have already mentioned that next-generation scintillator detectors may be built at two different sites, e.g. one in Europe and another in Hawaii, for the purpose of geo-neutrino research. In this case, the most interesting case is that at least one detector sees a shadowed signal. The generalization of the previous formulae to this case is straightforward.

Our results are reported in Table 2 for the Earth-crossing case and in Table 3 for core crossing. The quantities listed in each cell at row  $i$  and column  $j$  are the following probabilities:

$$\begin{aligned}
 P(i, \bar{j}) & \text{ Detector } i \text{ shadowed, } j \text{ not shadowed ;} \\
 P(\bar{i}, j) & \text{ Detector } i \text{ not shadowed, } j \text{ shadowed ;} \\
 P(i, j) & \text{ Both detectors shadowed .}
 \end{aligned}
 \tag{30}$$

For example, in Table 2 in the row ‘‘Pyhäsalmi’’ and column ‘‘South Pole’’ we read that the probability that a SN will be shadowed at Pyhäsalmi but not at the South Pole is 0.519, for the reverse case is 0.353, whereas the chance that both detectors see it shadowed is 0.062.

For the special case where one of the sites is the South Pole, it is intuitively obvious that Pyhäsalmi is the best location among the proposed ones, being farthest at north. For the most conservative scenario, in which no new large detectors will be built, the combination of IceCube at the South Pole plus Super-Kamiokande detector already existing in Japan offers a 73% probability that a comparison between a shadowed and an un-shadowed neutrino signal could be observed, and 17% probability for this comparison in the case of core shadowing. Notice that the case of a detector in Pyhäsalmi and

**Table 2.** Shadowing probability for two detectors. The quantities reported in each cell are explained in Eq. (30).

LOCATIONS	South Pole	Sydney	Hawaii	Kamioka	Fréjus	Soudan
Pyhäsalmi	.519	.457	.285	.179	.065	.148
	.353	.315	.231	.157	.052	.139
	.062	.130	.296	.400	.516	.433
Soudan	.475	.437	.187	.221	.162	
	.317	.310	.142	.208	.158	
	.097	.135	.386	.351	.410	
Fréjus	.461	.484	.326	.230		
	.307	.361	.285	.220		
	.107	.084	.242	.339		
Kamioka	.435	.278	.184			
	.290	.164	.152			
	.124	.281	.375			
Hawaii	.362	.251				
	.249	.168				
	.165	.277				
Sydney	.160					
	.129					
	.285					

**Table 3.** Same as Table 2 for core shadowing.

LOCATIONS	South Pole	Sydney	Hawaii	Kamioka	Fréjus	Soudan
Pyhäsalmi	.115	.116	.115	.116	.041	.110
	.064	.069	.082	.114	.035	.107
	.000	.000	.000	.000	.074	.005
Soudan	.112	.112	.107	.112	.111	
	.064	.069	.077	.104	.108	
	.000	.000	.005	.000	.001	
Fréjus	.110	.110	.110	.110		
	.064	.007	.082	.104		
	.000	.000	.000	.000		
Kamioka	.104	.104	.100			
	.064	.069	.078			
	.000	.000	.003			
Hawaii	.082	.082				
	.064	.069				
	.000	.000				
Sydney	.062					
	.057					
	.006					

another one in Hawaii, which is of importance for geo-neutrino research, offers also a nice opportunity for Earth effect detection in SN neutrinos. The probability that exactly one of them is in a shadowed position exceeds 50% (20% for core shadowing), whereas the probability that one or both are shadowed is about 80% (20% for core shadowing).

#### 4. Conclusions

The possibility to detect Earth matter effects in the neutrino signal from the next Galactic SN is a powerful tool to probe the neutrino mass hierarchy. Next-generation large volume detectors with excellent energy resolution would offer the opportunity to detect directly the specific signature of an energy-dependent modulation of the measured neutrino flux. Even if current detectors could not reconstruct directly these modulations, the comparison of the neutrino signal in a shadowed with an unshadowed detector could allow one to detect Earth effects. Of course, it is assumed that the location of the SN in the sky can be determined by observations in the electromagnetic spectrum. In the unlikely case that this is not possible, neutrinos alone can be enough to determine the SN location with sufficient precision [41, 42].

Motivated by these opportunities, we have provided the first detailed study of the probability that a detector at a given geographic latitude will observe a Galactic SN

in an Earth-shadowed or core-shadowed position. We have shown that this probability is rather insensitive to detailed assumptions about the uncertain distribution of core-collapse events in the Galaxy. The main effect is the simple geometric constraint that SNe occur within the Galactic disk.

We find that a far-northern location such as the Pyhäsalmi mine in Finland, the preferred site for the LENA scintillator detector, is almost optimal for observing a SN signal shadowed by the Earth. The shadowing probability is close to 60%, against an average of 50% for a random location on the Earth. The shadowing probability  $P_0(\lambda)$  depends only mildly on the latitude  $\lambda$  for  $\lambda > 40^\circ$ , a condition fulfilled by most of the northern locations proposed for next-generation experiments. The behavior for core shadowing is similar, although the advantage of a northern site is more pronounced. The core-crossing probability varies by almost a factor of two between a far southern and a far northern site, where it reaches almost 12%.

We have also studied the case of two detectors. It is of interest because one may be able to compare a shadowed with an unshadowed SN neutrino signal and thus diagnose Earth effects even if both detectors lack the energy resolution that is necessary to observe a modulated signal. On the other hand, if both detectors see a shadowed signal one may perform Earth tomography because the observed neutrinos would cross different geophysical layers [43]. For the South Pole, where IceCube will be completed in a few years, combined with Kamioka the probability that at least one of them is shadowed is almost 75%, for the South Pole combined with Pyhäsalmi it is almost 90%.

One particular scenario consists of a large-volume scintillator detector located at Pyhäsalmi to measure the geo-neutrino flux in a continental location and another such detector in Hawaii to measure it in an oceanic location. The probability that exactly one of them is shadowed exceeds 50% whereas the probability that one or both are shadowed is about 80%. Therefore, Pyhäsalmi and Hawaii are not only complementary for the purpose of geo-neutrino observations, but also for observing Earth matter effects in SN neutrinos.

The various probabilities relevant for two detectors at arbitrary locations are difficult to represent in a useful figure or table. Therefore, based on our benchmark Galactic SN distribution we provide an online tool that allows one to calculate the various Earth and core-shadowing probabilities for one or two detectors at arbitrary geographic locations [26].

## Acknowledgments

We thank Lothar Oberauer for interesting discussions in the initial stage of this work. We thank John Beacom, Eligio Lisi, Cecilia Lunardini and Daniele Montanino for careful reading the manuscript and for valuable suggestions and comments. Moreover, we thank Roberto Mirizzi for help with designing the online tool. This work was partially supported by the European Union under the ILIAS project, contract No. RII3-CT-2004-506222 and by the Deutsche Forschungsgemeinschaft under Grant No. SFB-375. The

work of A.M. is supported in part by the Italian “Istituto Nazionale di Fisica Nucleare” (INFN) and by the “Ministero dell’Istruzione, Università e Ricerca” (MIUR) through the “Astroparticle Physics” research project.

## References

- [1] E. Cappellaro, R. Evans and M. Turatto, “A new determination of supernova rates and a comparison with indicators for galactic star formation,” *Astron. Astrophys.* **351** (1999) 459 [astro-ph/9904225].
- [2] R. Diehl *et al.*, “Radioactive  $^{26}\text{Al}$  and massive stars in the Galaxy,” *Nature* **439** (2006) 45 [astro-ph/0601015].
- [3] S. Woosley and T. Janka, “The physics of core-collapse supernovae,” *Nature Physics* **1** (2005) 147 [astro-ph/0601261].
- [4] G. G. Raffelt, “Particle physics from stars,” *Annu. Rev. Nucl. Part. Sci.* **49** (1999) 163 [hep-ph/9903472].
- [5] A. S. Dighe and A. Y. Smirnov, “Identifying the neutrino mass spectrum from the neutrino burst from a supernova,” *Phys. Rev. D* **62** (2000) 033007 [hep-ph/9907423].
- [6] C. Lunardini and A. Yu. Smirnov, “Supernova neutrinos: Earth matter effects and neutrino mass spectrum,” *Nucl. Phys. B* **616** (2001) 307 [hep-ph/0106149].
- [7] C. Lunardini and A. Y. Smirnov, “Probing the neutrino mass hierarchy and the 13-mixing with supernovae,” *JCAP* **0306** (2003) 009 [hep-ph/0302033].
- [8] A. S. Dighe, M. T. Keil and G. G. Raffelt, “Detecting the neutrino mass hierarchy with a supernova at IceCube,” *JCAP* **0306** (2003) 005 [hep-ph/0303210].
- [9] K. Takahashi and K. Sato, “Effects of neutrino oscillation on supernova neutrino: Inverted mass hierarchy,” *Prog. Theor. Phys.* **109** (2003) 919 [hep-ph/0205070].
- [10] S. H. Chiu and T. K. Kuo, “Probing neutrino mass hierarchies and  $\theta_{13}$  with supernova neutrinos,” *Phys. Rev. D* **73** (2006) 033007 [Erratum-*ibid.* **D 73** (2006) 059901].
- [11] B. Jegerlehner, F. Neubig and G. Raffelt, “Neutrino oscillations and the supernova 1987A signal,” *Phys. Rev. D* **54** (1996) 1194 [astro-ph/9601111].
- [12] G. G. Raffelt, “Mu- and tau-neutrino spectra formation in supernovae,” *Astrophys. J.* **561** (2001) 890 [astro-ph/0105250].
- [13] M. T. Keil, G. G. Raffelt and H. T. Janka, “Monte Carlo study of supernova neutrino spectra formation,” *Astrophys. J.* **590** (2003) 971 [astro-ph/0208035].
- [14] G. G. Raffelt, M. T. Keil, R. Buras, H. T. Janka and M. Rampp, “Supernova neutrinos: Flavor-dependent fluxes and spectra,” *Proc. of the 4th Workshop on Neutrino Oscillations and their Origin: NooN 2003* (10–14 February 2003, Kanazawa, Japan), ed. by Y. Suzuki *et al.* (World Scientific, Singapore, 2004), pp. 380–387 [astro-ph/0303226].
- [15] M. Kachelriess, R. Tomàs, R. Buras, H. T. Janka, A. Marek and M. Rampp, “Exploiting the neutronization burst of a galactic supernova,” *Phys. Rev. D* **71** (2005) 063003 [astro-ph/0412082].
- [16] R. C. Schirato, G. M. Fuller, “Connection between supernova shocks, flavor transformation, and the neutrino signal,” astro-ph/0205390.
- [17] R. Tomàs, M. Kachelriess, G. Raffelt, A. Dighe, H. T. Janka and L. Scheck, “Neutrino signatures of supernova shock and reverse shock propagation,” *JCAP* **0409** (2004) 015 [astro-ph/0407132].
- [18] G. L. Fogli, E. Lisi, A. Mirizzi and D. Montanino, “Probing supernova shock waves and neutrino flavor transitions in next-generation water-Cherenkov detectors,” *JCAP* **0504** (2005) 002 [hep-ph/0412046].
- [19] G. L. Fogli, E. Lisi, A. Mirizzi and D. Montanino, “Damping of supernova neutrino transitions in stochastic shock-wave density profiles,” hep-ph/0603033.



- [20] A. S. Dighe, M. T. Keil and G. G. Raffelt, “Identifying earth matter effects on supernova neutrinos at a single detector,” *JCAP* **0306** (2003) 006 [hep-ph/0304150].
- [21] A. S. Dighe, M. Kachelriess, G. G. Raffelt and R. Tomàs, “Signatures of supernova neutrino oscillations in the earth mantle and core,” *JCAP* **0401** (2004) 004 [hep-ph/0311172].
- [22] L. Oberauer, F. von Feilitzsch and W. Potzel, “A large liquid scintillator detector for low-energy neutrino astronomy,” *Nucl. Phys. Proc. Suppl.* **138** (2005) 108.  
See also <http://www.e15.physik.tu-muenchen.de/research/lena.html>
- [23] T. Araki *et al.*, “Experimental investigation of geologically produced antineutrinos with KamLAND,” *Nature* **436** (2005) 499.
- [24] Centre for Underground Physics in Pyhäsalmi (CUPP), <http://cupp oulu.fi>
- [25] S. Dye, “Hanohano,” talk at *Neutrino Sciences 2005–Neutrino Geophysics* (Honolulu, Hawaii, 2006), <http://www.phys.hawaii.edu/~jelena/post/hnsc/HawaiiAnti-NeutrinoObservatory.ppt>
- [26] Online tool for calculating Earth-shadowing probabilities of supernova neutrinos, <http://www.mppmu.mpg.de/supernova/shadowing>
- [27] K. M. Ferriere, “The interstellar environment of our Galaxy,” *Rev. Mod. Phys.* **73** (2001) 1031 [astro-ph/0106359].
- [28] D. F. Figer, R. M. Rich, S. S. Kim, M. Morris and E. Serabyn, “An extended star formation history for the Galactic Center from Hubble Space Telescope/NICMOS observations,” *Astrophys. J.* **601** (2004) 319 [astro-ph/0309757].
- [29] I. Yusifov and I. Küçük, “Revisiting the radial distribution of pulsars in the Galaxy,” *Astron. Astrophys.* **422** (2004) 545 [astro-ph/0405559].
- [30] D. R. Lorimer, “The Galactic population and birth rate of radio pulsars,” in: *Young neutron stars and their environments*, IAU Symposium No. 218 (14–17 July 2003, Sydney, Australia), ed. by F. Camilo and B. M. Gaensler (San Francisco, Astronomical Society of the Pacific, 2004) p. 105 [astro-ph/0308501].
- [31] K. R. Lang, *Astrophysical Formulae*, (Springer-Verlag, Berlin, 1980).
- [32] S. T. Petcov, “Diffractive-like (or parametric-resonance-like?) enhancement of the Earth (day-night) effect for solar neutrinos crossing the Earth core,” *Phys. Lett. B* **434** (1998) 321 [hep-ph/9805262].
- [33] E. K. Akhmedov, “Parametric resonance of neutrino oscillations and passage of solar and atmospheric neutrinos through the earth,” *Nucl. Phys. B* **538** (1999) 25 [hep-ph/9805272].
- [34] F. D. Stacey, *Physics of the Earth*, 2nd Edition (John Wiley & Sons, New York, 1977).
- [35] Y. Fukuda *et al.*, “The Super-Kamiokande detector,” *Nucl. Instrum. Meth. A* **501**, (2003) 418.  
See also <http://www-sk.icrr.u-tokyo.ac.jp/sk>
- [36] J. Ahrens *et al.* [IceCube Collaboration], “IceCube: The next generation neutrino telescope at the South Pole,” *Nucl. Phys. Proc. Suppl.* **118** (2003) 388 [astro-ph/0209556]. See also <http://icecube.wisc.edu>
- [37] C. K. Jung, “Feasibility of a next generation underground water Cherenkov detector: UNO,” hep-ex/0005046. See also <http://ale.physics.sunysb.edu/uno>
- [38] K. Nakamura, “Hyper-Kamiokande: A next generation water Cherenkov detector,” *Int. J. Mod. Phys. A* **18** (2003) 4053.
- [39] J. E. Campagne, M. Maltoni, M. Mezzetto and T. Schwetz, “Physics potential of the CERN-MEMPHYS neutrino oscillation project,” hep-ph/0603172.  
See also [http://apc-p7.org/APC\\_CS/Experiences/MEMPHYS/index.html](http://apc-p7.org/APC_CS/Experiences/MEMPHYS/index.html)
- [40] L. Oberauer, “LENA,” talk at *NO-VE 2006*, 3rd International Workshop on Neutrino Oscillations in Venice (Venice, Italy, 2006), [http://axpd24.pd.infn.it/NO-VE2006/talks/NOVE\\_Oberauer.ppt](http://axpd24.pd.infn.it/NO-VE2006/talks/NOVE_Oberauer.ppt).
- [41] J. F. Beacom and P. Vogel, “Can a supernova be located by its neutrinos?,” *Phys. Rev. D* **60** (1999) 033007 [astro-ph/9811350].
- [42] R. Tomàs, D. Semikoz, G. G. Raffelt, M. Kachelriess and A. S. Dighe, “Supernova pointing with low- and high-energy neutrino detectors,” *Phys. Rev. D* **68** (2003) 093013 [hep-ph/0307050].

- [43] M. Lindner, T. Ohlsson, R. Tomàs and W. Winter, “Tomography of the Earth’s core using supernova neutrinos,” *Astropart. Phys.* **19** (2003) 755 [hep-ph/0207238].